Journal of Hazardous Materials 194 (2011) 193–201

Contents lists available at ScienceDirect

Journal of Hazardous Materials

journal homepage: www.elsevier.com/locate/jhazmat

Removal of Ag^+ from water environment using a novel magnetic thiourea-chitosan imprinted Ag^+

Lulu Fan, Chuannan Luo*, Zhen Lv, Fuguang Lu, Huamin Qiu

College of Chemistry and Chemical Engineering, University of Jinan, Jinan 250022, China

ARTICLE INFO

Article history:
Received 29 April 2011
Received in revised form 18 July 2011
Accepted 24 July 2011
Available online 6 August 2011

Keywords:
Thiourea-chitosan
Magnetite
Langmuir
Adsorption
Ag^+

ABSTRACT

A novel, thiourea-chitosan coating on the surface of magnetite (Fe_3O_4) (Ag-TCM) was successfully synthesized using Ag(I) as imprinted ions for adsorption and removal of Ag(I) ions from aqueous solutions. The thermal stability, chemical structure and magnetic property of the Ag-TCM were characterized by the scanning electron microscope (SEM), Fourier transform infrared spectrometer (FT-IR) and vibrating sample magnetometer (VSM), respectively. Batch adsorption experiments were performed to evaluate the adsorption conditions, selectivity and reusability. The results showed that the maximum adsorption capacity was 4.93 mmol/g, observed at pH 5 and temperature 30 °C. Equilibrium adsorption was achieved within 50 min. The kinetic data, obtained at the optimum pH 5, could be fitted with a pseudo-second order equation. Adsorption process could be well described by Langmuir adsorption isotherms and the maximum adsorption capacity calculated from Langmuir equation was 5.29 mmol/g. The selectivity coefficient of Ag(I) ions and other metal cations onto Ag-TCM indicated an overall preference for Ag(I) ions, which was much higher than non-imprinted thiourea-chitosan beads. Moreover, the sorbent was stable and easily recovered, the adsorption capacity was about 90% of the initial saturation adsorption capacity after being used five times.

1. Introduction

Contamination of aquatic media by heavy metals is a serious environmental problem, mainly due to the discharge of industrial waste. Heavy metals are highly toxic at low concentrations and can accumulate in living organisms, causing several disorders and diseases [1–3]. Among the many methods available for the removal of heavy metals from aqueous solution are electrochemical precipitation, ion exchange, ultrafiltration, and reverse osmosis [4–11]. Adsorption techniques have been shown to be a feasible option, both technically and economically. Chitosan has been reported to have high potential for adsorption of metal ions [12–16]. To improve their absorption capacity and enhance the separation rate [17–21], the design and exploration of novel adsorbents are still necessary [22–24]. Recent research has been focused on the modification of chitosan for enhanced adsorption performance based on introducing chemical groups, like thiourea [25,26], which can offer more $-NH_2$. In addition, magnetic fluids have the capability to treat large amounts of wastewater within a short time and can be conveniently separated from wastewater; at the same time, they could be tailored by using functionalized polymers, novel molecules, or inorganic materials to impart surface reactivity. Coating thiourea-chitosan with magnetic fluids is a new method to expand function of the chitosan, and the method has been reported that it can improve the surface area for adsorption and reduce the required dosage for the adsorption of metal ions [27,28].

Surface imprinting technology is an emerging technology that has attracted much attention in generating recognition sites by reversible immobilization of template molecules on cross-linked macromolecular polymer matrixes. Molecularly imprinted polymers represent a new class of materials possessing high selectivity and good affinity for target molecules [29,30]. Ion imprinted polymers have shown great promise as a method for preparing materials, which are capable of ion recognition [31]. So far, a lot of metal ion imprinted polymers have been prepared, including Pd(II) [32], Cu(II) [33], Zn(II) [34], Ni(II) [35], As(III)[29], Ca(II) [36] and Mg(II) [37] imprinted ones, however, surface imprinting magnetic chitosan of Ag^+ has not been synthesized and applied in selective removing Ag^+ from aqueous solution. The preparation of Ag-TCM is schematically illustrated in Scheme 1.

In this work, thiourea-chitosan coating on the surface of magnetite (Fe_3O_4), which were using Ag(I) as imprinted ions (Ag-TCM) was successfully synthesized, and applied to removing Ag^+ from wastewater. The resulting functional material is easily separated due to the magnetism. Furthermore, high removal efficiency and selectivity in adsorbing Ag^+ can be achieved by applying the Ag-TCM. This information will be useful for further applications in the treatment of practical waste effluents.

* Corresponding author. Fax: +86 53182765491.
E-mail addresses: fanlu1949@126.com (L. Fan), chm_luocn@ujn.edu.cn (C. Luo).

0304-3894/$ – see front matter © 2011 Elsevier B.V. All rights reserved.
doi:10.1016/j.jhazmat.2011.07.080

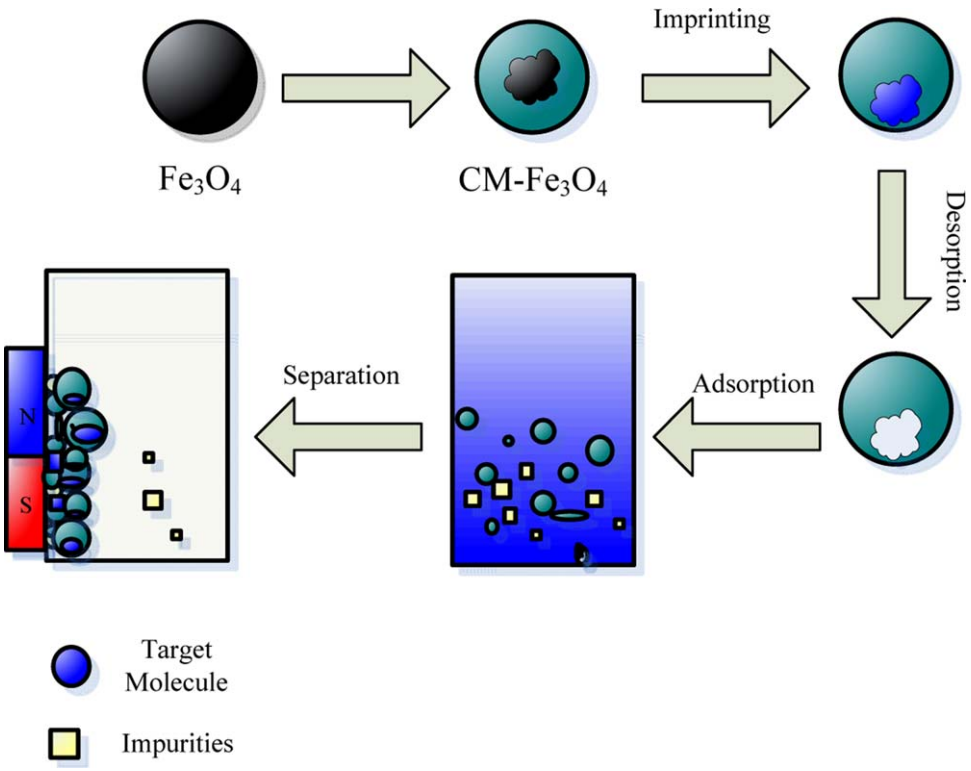

Scheme 1. Synthesis route of Ag-TCM and their application for removal of Ag^+ with the help of an external magnetic field.

2. Materials and methods

2.1. Materials

Chitosan with 80 mesh, 96% degree of deacetylation and average-molecular weight of 6.36×10^5 was purchased from Qingdao Baicheng Biochemical Corp. (China). $FeCl_3{\cdot}6H_2O$ and $FeCl_2{\cdot}4H_2O$ were purchased from Damao Chemical Agent Company (Tijin, China). Ag(I) standard solution was obtained from National Steel Material Test Center (Beijing, China). Glutaradehyde, epichlorohydrin, 3% acetic solution and thiourea were Aldrich products. All other reagents used in this study were analytical grade, and distilled or double distilled water was used in the preparation of all solutions.

2.2. Preparation of magnetic thiourea-chitosan

1.7312 g of $FeCl_3{\cdot}6H_2O$, 0.6268 g of $FeCl_2{\cdot}4H_2O$ and 25 mL of double distilled water were dropwise to ammonia solution, which was purged with nitrogen and stirred in a water bath at 95 °C for 2 h. Magnetic particles used in the chitosan coating were obtained by magnetic separation [15].

Thiourea-chitosan was prepared following the method of Zhou et al. [38]. 2 mL epichlorohydrin was dissolved in 100 mL of acetone, 1 g chitosan microspheres were added, and the mixture was mixed at 30 °C for 24 h. 1 g thiourea was added, and stirring was continued for 6 h at 60 °C, followed by addition of further thiourea (2 g) with stirring at 60 °C. NaOH (1 M, 50 mL) was added, and the slurry was agitated (4 h, 60 °C). The solid product (thiourea-chitosan) was filtered and successively washed with acetone, deionized water, and methanol, and dried in a vacuum oven at 65 °C. The synthesis is shown in Scheme 2.

0.5 g thiourea-chitosan flake was dissolved in 50 mL 3% of acetic solution to give a final concentration of 1.5% (w/v). 0.2 g Magnetic particles were added in the thiourea-chitosan solution in a four-neck rounded bottom flask. After ultrasonic dispersion, some liquid paraffin and Span-80 were added in the solution. The solution's pH was adjusted to maintain a level of 8.0–9.0 by adding 25% (v/v)

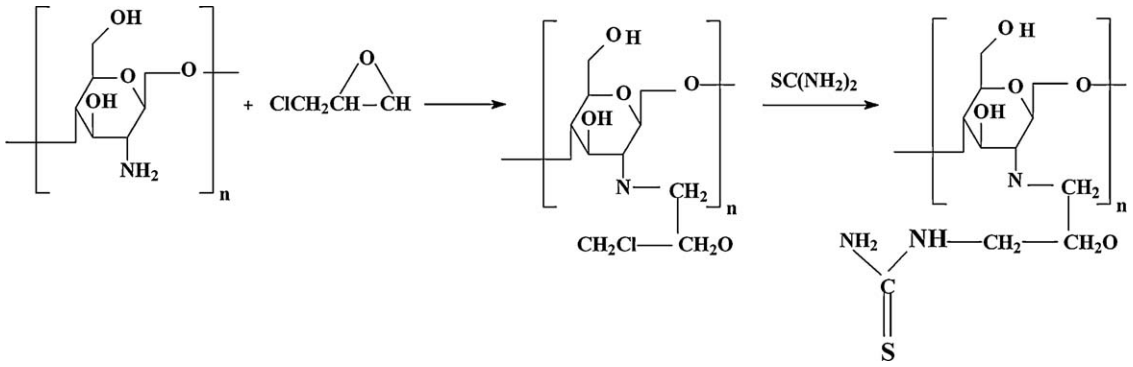

Scheme 2. Schematic depiction of the formation of thiourea-chitosan particles.

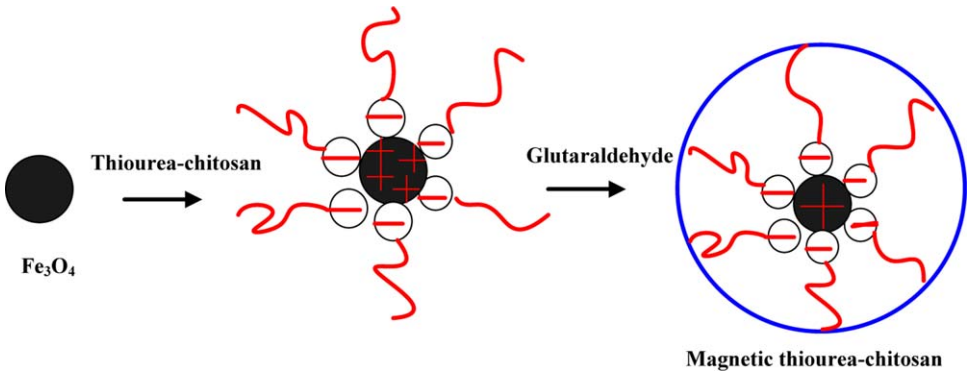

Scheme 3. Schematic depiction of the formation of magnetic thiourea-chitosan.

ammonium hydroxide solution during the reaction. After the above steps, 2.0 mL of pure glutaraldehyde was added into reaction flask to mix with the solution and was stirred at 60 °C for 2 h. The precipitate was washed with petroleum ether, ethanol and distilled water in turn until pH was about 7. Then, the precipitate was dried in a vacuum oven at 50 °C. The obtained product was magnetic thiourea-chitosan. The synthesis is shown in Scheme 3.

2.3. Preparation of Ag-TCM

Magnetic thiourea-chitosan and Ag(I) were added in a flask and dispersed in distilled water by ultrasonic dispersion for 30 min. Some of epichlorohydrin was added. The mixture solution was stirred for 4 h, and then was at 30 °C for 24 h. And then, the beads were extensively washed with petroleum ether, ethanol and distilled water in sequence to remove any unreacted fraction. Finally, the template ions were removed from the polymer beads using 0.5 mol/L HNO_3. The procedure was repeated several times until the template ions could not be detected in the filtrate. The beads were added into 0.1 mol/L NaOH aqueous solution for 5–8 h to active amino group and then were dried under vacuum oven at 50 °C. Thus, the thiourea-chitosan coating on the surface of magnetite with Ag(I) as template ions was obtained. As a control, the non-imprinted magnetic thiourea-chitosan (TCM) was also prepared under identical conditions without adding Ag(I) [29].

2.4. Batch adsorption experiments

Batch adsorption experiments were carried out in 100 mL Erlenmeyer flasks. The amount of adsorbent used was 0.1 g and the volume of aqueous solution was maintained at 20.0 mL. The pH of the aqueous solution was adjusted by adding 0.1 mol/L NaOH or 0.1 mol/L HNO_3 and was measured using a pH meter (pH 510, Kesheng, Shenzhen). The batch experiments were carried out at a constant temperature maintained at 30 °C for 50 min. After adsorption equilibration, the adsorbent was separated by external magnetic field. Ag(I) concentration of the magnetic separation was measured with a flame atomic absorption spectrophotometer (AA-6200, Shimadzu Ins), equipped with a hydride vapor generator (HVG-1, Shimadzu Ins) (HVG-FAAS) at 200 nm wavelengths, using 0.1 mol/L HNO_3 solution as reducing reagent. The concentration of other metal ions was measured with FAAS.

The amount of Ag(I) ions adsorbed per unit mass of Ag-TCM was calculated from the following equation:

$$Q = \frac{(C_0 - C_e)V}{W}, \quad E = \frac{C_0 - C_e}{C_0} \times 100\%$$

where C_0 and C_e are the initial and equilibrium concentrations of Ag^+ in milligrams per liter, respectively, V is the volume of Ag^+ solution, in liters, and W is the weight of the adsorbent used, in grams.

2.5. Selective determination

The selectivity of Ag-TCM and TCM for Ag(I) ions over other metal ions were evaluated from the selectivity coefficient K, which was determined by incubating 0.5 g of beads with each individual heavy metal ions present in 50 mL of distilled water under identical conditions.

The selectivity coefficient is defined as:

$$K_1 = \frac{Q_1}{Q_2}$$

Q_1 (adsorption capacity of Ag^+), Q_2 (adsorption capacity of different ions).

2.6. Desorption and regeneration studies

The desorption study is very important since the regeneration of adsorbent decides the economic success of the adsorption process. In this study, several solvents/solutions were tried to regenerate the biosorbents. 0.1 mol/L HNO_3 aqueous solution was found effective in desorbing Ag(I) from the loaded adsorbents. The beads was regenerated using 0.1 mol/L HNO_3 solution, the procedure was repeated for many times until Ag(I)could not be detected in the filtrate. Then, Ag-TCM was washed thoroughly with distilled water to a neutral pH. The regenerated Ag-TCM was reused in the following adsorption experiments and the procedure was repeated for 5 times by using the same Ag-TCM.

2.7. Characterization of the samples

Microscopic observation of magnetic particles, magnetic thiourea-chitosan and dried Ag-TCM was carried out by using a scanning electron microscope (S-2500, Japan Hitachi). FTIR spectra were measured on a Nicolet, Magna 550 spectrometer. The magnetic thiourea-chitosan was mixed with KBr and pressed to a pellet for measurement. A vibrating-sample magnetometer (VSM) (MAG-3110, Freescale) was used at room temperature to characterize the magnetic properties of Ag-TCM.

3. Results and discussion

3.1. Characterization of Ag-TCM

The morphology of Ag-TCM was observed by SEM. As shown in Fig. 1, the well shaped particles with diameter distribution from 20 to 100 nm were achieved. Majority of the particles are spherical.

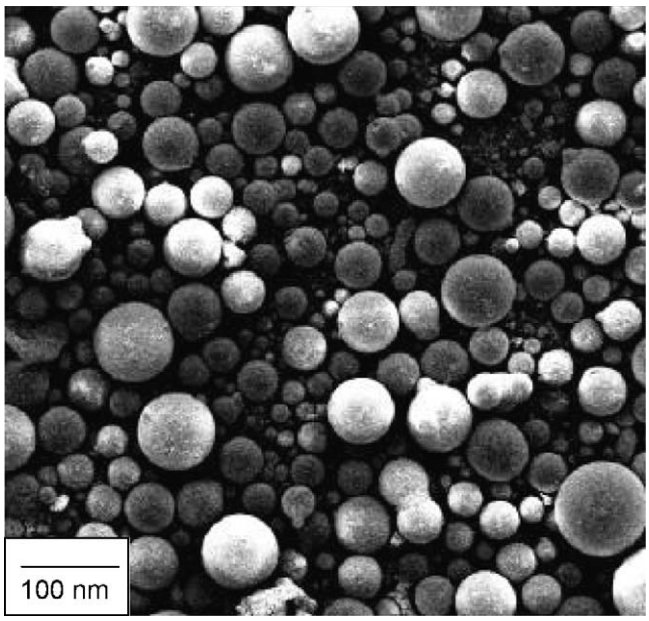

Fig. 1. Scanning electron microscope of Ag-TCM.

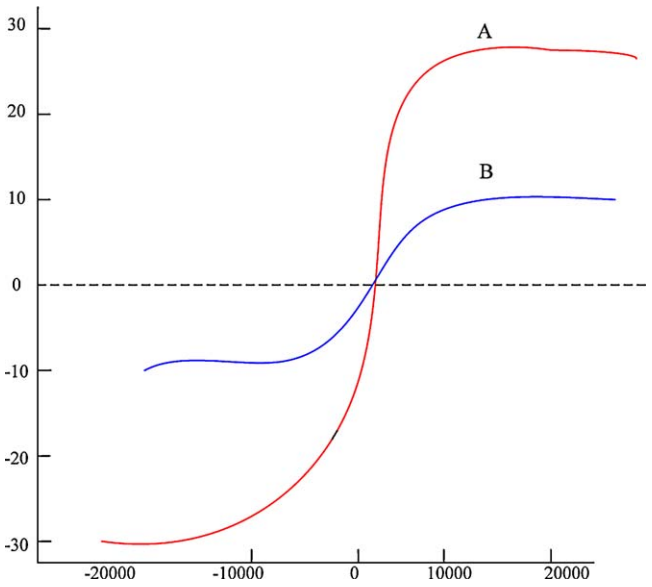

Fig. 3. VSM magnetization curves of magnetic particles and Ag-TCM (A: magnetic particles, *S*, saturation magnetization is 31.5 emu/g; B: Ag-TCM, *S*, saturation magnetization is 10.16 emu/g).

Spherical molecular imprinting polymers have large surface area, indicating that large number of effective imprinting sites could exist in the surface to rebind the template molecules in aqueous media.

The physical property analyses of chitosan and Ag-TCM are important in this study because the analyses give some insights of the effect of cross-linking reactions to the natural chemical and physical properties of chitosan. This information is very useful in elucidating the adsorption capacity of the adsorbents towards adsorbates. The surface areas of Ag-TCM and chitosan were determined by nitrogen sorption measurements [39]. The surface areas of Ag-TCM and chitosan were 7.51 and 14.2 m^2/g, respectively. The surface area of chitosan decreased with cross-linking modification. The relative adsorption performance of different adsorbent is highly dependent on the internal pore structure of each material. Therefore, crosslinking modification offers some attractive advantages. It is not only able to increase the surface area and average pore diameter, but also reinforce the chemical strength of adsorbents in acidic medium.

Infrared spectra of thiourea-chitosan (A) and Ag-TCM (B) samples are shown in Fig. 2. The adsorption band around 3420 cm^{-1}, revealing the stretching vibration of N–H group bonded with O–H group in chitosan, and at 1661 cm^{-1} confirms the N–H scissoring from the primary amine, due to the free amino groups in the crosslinked chitosan. The band around 1065 cm^{-1} is attributed to the combined effects of C–N stretching vibration of primary amines and the C–O stretching vibration from the primary alcohol in chitosan. The spectrum of both displays bands near 1548 cm^{-1} which are assigned to ν C–N of thiourea moiety. The new peak of Ag-TCM in Fig. 2(B) is displayed near 580 cm^{-1}(characteristic peak of Fe_3O_4), which demonstrates that a layer of modified chitosan was formed on the surface of magnetite particles.

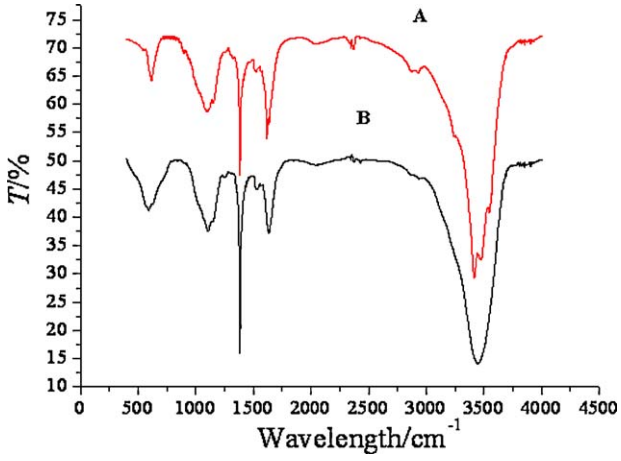

Fig. 2. IR spectra of thiourea-chitosan (A), and Ag-TCM (B).

The magnetization measurement performed with VSM (Fig. 3) indicated that the saturation magnetization of the magnetic particles was 31.5 emu/g. As mentioned in a previous report, this magnetic susceptibility value is sufficient for this adsorbent to be used in wastewater treatment [2]. A saturation magnetization of 31.5 emu/g is obtained on the magnetic particles which decreases to 10.16 emu/g due to the shielding of the polymeric coating resulting from the modification process. However, the Ag-TCM with declined saturation magnetization value also posses enough magnetic response to meet the need of magnetic separation.

XRD patterns of pure Fe_3O_4, TCM and Ag-TCM are shown in Fig. 4, indicating the existence of iron oxide particles (Fe_3O_4), which has magnetic properties and can be used for the magnetic separation. The XRD analysis results of pure Fe_3O_4, TCM and Ag-TCM were mostly coincident. Six characteristic peaks for Fe_3O_4 ($2\theta = 30.1^\circ$, 35.5°, 43.3°, 53.4°, 57.2° and 62.5°), marked by their indices ((2 2 0), (3 1 1), (4 0 0), (4 2 2), (5 1 1), and (4 4 0)), were observed in three samples.

3.2. Effect of pH on the adsorption process

The pH of the aqueous solution, the most important parameter on adsorption studies, strongly affects the adsorption property of beads for heavy metal ions. Metal ions are pH-dependently adsorbed onto non-specific and specific sorbents [40]. The adsorption process of metal ions is sensitive to pH and usually do not occur at low pH [41].

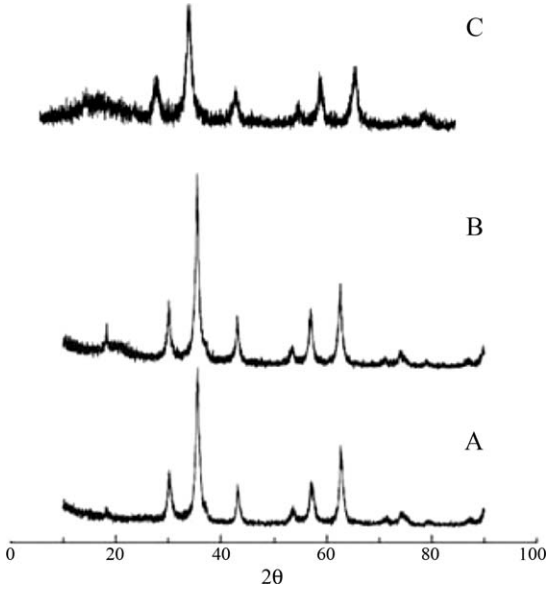

Fig. 4. XRD pattern of Fe_3O_4 (A), TCM (B) and Ag-TCM (C).

Hence, the effect of pH on the chelation between Ag-TCM and Ag was investigated over the range from 3.0 to 7.0, and the results are shown in Fig. 5.

As indicated in Fig. 5, the uptake capacity of Ag^+ increased when the solution pH was raised from 3.0 to 5.0. The maximum adsorption values for Ag(I) ions onto Ag-TCM and TCM were 4.6 mmol/g and 2.46 mmol/g dry beads at pH 5, respectively, from which the imprinting effect was greatly observed. This could be explained by the fact that, at a lower pH, the amine groups on surface of Ag-TCM can be easily protonated, inducing an electrostatic repulsion of Ag^+. That is because the functional groups of inserted thiourea moieties, which are the most effective ones, on the biomass surfaces offers more metal adsorption sites. This may be attributed to the presence of free lone pair of electrons on nitrogen atoms suitable for coordination with the metal ions to give the corresponding resin–metal complex. The slight decrease of the uptake in the acidic media may be attributed to the protonation of the lone pair of nitrogen that hinders the complex formation. The uptake of Ag^+ beyond the natural pH (pH > 5) is attributed to the formation of metal hydroxide species such as soluble Ag^+ and/or insoluble precipitate of Ag(OH). Hence, pH 5 was chosen as the optimal pH in the following experiments.

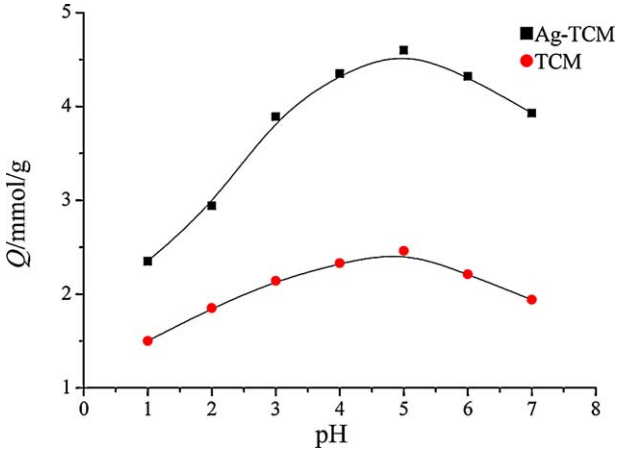

Fig. 5. Effect of pH on the adsorption capacity (initial concentration, 20 mmol/L; temperature, 303 K; contact time, 50 min).

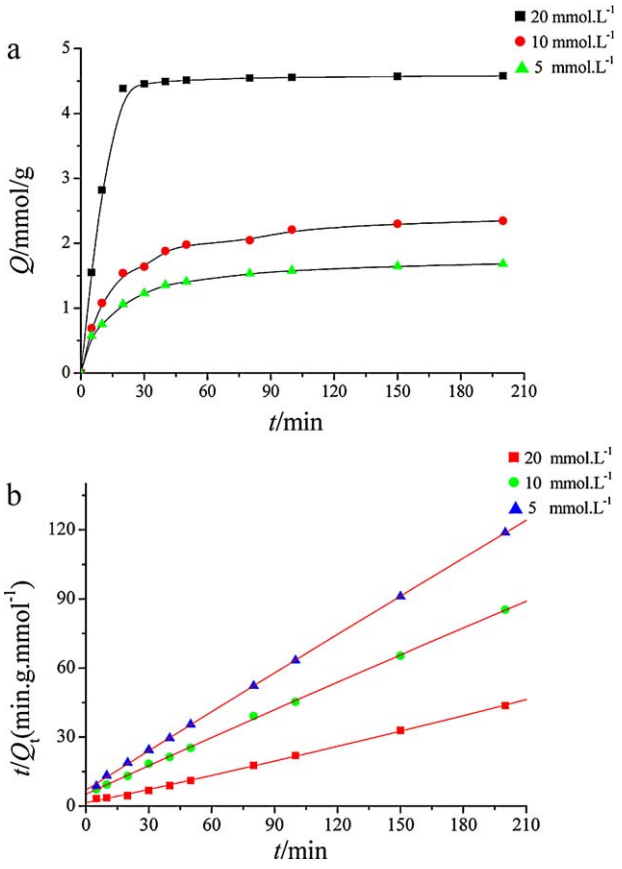

Fig. 6. (a) Effect of contact time on Ag^+ adsorption by Ag-TCM; (b) pseudo-second-order kinetics for adsorption of Ag^+ (pH 5, temperature: 303 K).

3.3. Adsorption kinetics

The effect of the contact time for Ag-TCM on the adsorption capacity for Ag^+ is described in Fig. 6. Obviously, adsorbent showed a good performance in adsorption during the first 30 min. The time required to achieve the adsorption equilibrium was only 50 min. There is no significant change from 1 h to 3 h.

The adsorption kinetics of Ag^+ onto Ag-TCM was investigated with the help of two kinetic models, namely the Lagergren pseudo-first-order and pseudo-second-order model. The Lagergren rate equation is one of the most widely used adsorption rate equations for the adsorption of solute from a liquid solution. The pseudo-first-order kinetic model is expressed by the following equation [42]:

$$\frac{dQ_t}{dt} = K_1 (Q_e - Q_t)$$

Integrating this equation for the boundary conditions $t = 0$ to $t = t$ and $Q = 0$ to $Q = Q_t$, gives:

$$\ln (Q_e - Q_t) = \ln Q_e - K_1 t$$

where Q_e and Q_t refer to the amount of Ag^+ adsorbed (mmol/g) at equilibrium and at any time, t (min), respectively, and K_1 is the equilibrium rate constant of pseudo-first-order sorption (1/min).

The slope and intercept of the plot of log $(Q_e - Q_t)$ versus t are used to determine the first-order rate constant, K_1. It was found that the correlation coefficient (R^2) has low value (<90%) for adsorbents for Ag^+ concentrations studied and a very large difference exists between Q (Experimental) and Q (Calculated), indicating a poor pseudo-first-order fit to the experimental data. The inapplicability of the pseudo-first-order model to describe the kinetics

Table 1
Adsorption kinetic parameters of Ag^+ onto Ag-TCM.

Initial conc. C_0 (mmol/mL)	Pseudo-first-order			Pseudo-second-order			
	K_1 (min^{-1})	$Q_{e,cal}$ (mmol/g)	R^2	$Q_{e,cal}$ (mmol/g)	K_2 (g/mmol/min)	$Q_{e,exp}$ (mmol/g)	R^2
5	0.0127	1.005	0.87	1.81	0.042	1.63	0.998
10	0.013	1.43	0.88	2.5	0.029	2.14	0.999
20	0.0148	0.977	0.5	4.7	0.051	4.6	0.998

of Ag^+ by adsorption using adsorbents was also observed in some previous work [43,44].

Another kinetic model is pseudo-second-order model, which is expressed by [45]:

$\frac{dQ_t}{dt} = K_2(Q_e - Q_t)^2$

Rearranging the variables gives

$$\frac{dQ_t}{(Q_e - Q_t)^2} = K_2 dt$$

Integrating this equation for the boundary conditions $t = 0$ to $t = t$ and $Q = 0$ to $Q = Q_t$, gives:

$$\frac{t}{Q_t} = \frac{1}{(K_2 Q_e^2)} + \frac{t}{Q_e}$$

where K_2 is the equilibrium rate constant of pseudo-second-order adsorption (g/mmol/min). The slope and intercept of the plot of t/Q_t versus t were used to calculate the second-order rate constant, K_2. The corresponding kinetic parameters from both models are listed in Table 1. The correlation coefficient (R^2) for the pseudo-second-order adsorption model has high value (>99%) for adsorbent. The calculated equilibrium adsorption capacity by Ag-TCM is 4.6 mmol/g, which is consistent with the experimental data (4.7 mmol/g) [46]. These facts suggest that the pseudo-second-order adsorption mechanism is predominant, and that the overall rate of the Ag^+ adsorption process appears to be controlled by the chemisorption process [47].

In addition, the optimum contact time for adsorption of Ag^+ appears to be 50 min. This can be attributed to the large surface area, the sufficient exposure of active sites and the high surface reactivity of the Ag-TCM. The sorption of Ag^+ is rapid during the initial stages of the sorption process, followed by a gradual process. In latter stages, however, the rate of Ag^+ adsorption becomes slower. It may be attribute to the great decrease of the bonding sites on the surface of Ag-TCM and the aggregation between particulates. The Ag^+ have to first encounter the boundary layer effect and then adsorb on the surface, and finally they have to diffuse into the porous structure of the adsorbent which takes a longer time.

3.4. Evaluation of adsorption isotherm models

The equilibrium adsorption isotherm is fundamental to describe the interactive behavior between the solution and the adsorbent and is important in designing an adsorption system. The widely used Langmuir model has been found to fit the process successfully. The equation can be expressed as

$$\frac{C_e}{Q} = \frac{1}{(K_L Q_0)} + \frac{C_e}{Q_0}$$

where C_e is the equilibrium concentration of metal ions in solution (mmol/L), Q is the adsorbed value of metal ions at equilibrium concentration (mmol/g), Q_0 the maximum adsorption capacity (mmol/g), and K_L is the Langmuir binding constant, which is related to the energy of adsorption. Plotting C_e/Q against C_e gives a straight line with slope and intercept equal to $1/Q_0$ and $1/(K_L\ Q_0)$, respectively. It is described in Fig. 7.

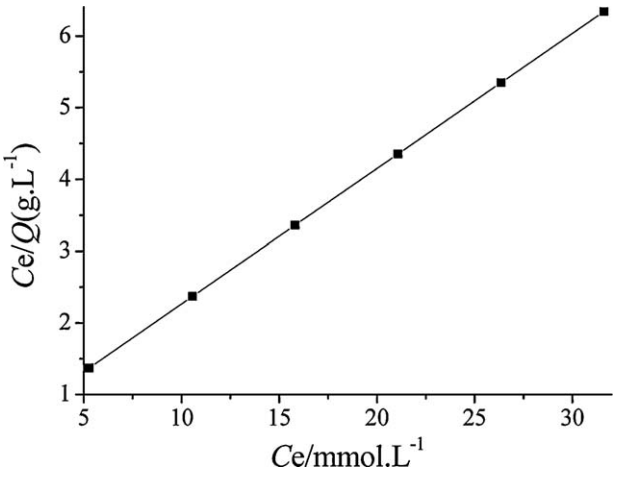

Fig. 7. The linear dependence of C_e/Q on C_e (pH 5; temperature, 303 K; contact time, 50 min).

By calculating, the results are as follows:

$$\frac{C_e}{Q} = 0.1887 C_e + 0.3774, \quad (R^2 = 0.9996),$$

$$Q_0 = 5.29\ \text{mmol/g},\ K_L = 0.5\ \text{L/mmol}$$

The values of Q_0 obtained from Langmuir curves are mainly consistent with that experimentally obtained (4.93 mmol/g), indicating that the adsorption process is mainly monolayer. The chelation adsorption mechanism for Ag^+ may give controlled monolayer adsorption.

Furthermore, the essential characteristics of the Langmuir isotherm can be described by a separation factor, which is defined by the following equation:

$$R_L = \frac{1}{1 + K_L C_e}$$

The value of R_L indicates the shape of the Langmuir isotherm and the nature of the adsorption process. It is considered to be a favorable process when the value is within the range 0–1. In our study, the value of R_L calculated for the initial concentrations of Ag^+ was 0.09. Since the result is within the range of 0–1, the adsorption of Ag^+ onto adsorbent appears to be a favorable process. In addition, the low R_L values (<0.1) implied that the interaction of Ag^+ with Ag-TCM might be relatively strong.

3.5. Effect of temperature on adsorption

The adsorption capacity of Ag-TCM for Ag(I) increased as the temperature is raised from 25 to 30 °C (Fig. 8), which was opposite to TCM. It was apparent that at the lower temperature (30 °C), the adsorption of Ag(I) onto Ag-TCM or the formation of Ag-TCM with Ag(I) complexes was favored. With the increase of temperature, Ag^+ ggot more energy to overcome electrostatic force between itself and Ag-TCM' surface, thus Ag^+ was easier to be adsorbed. In

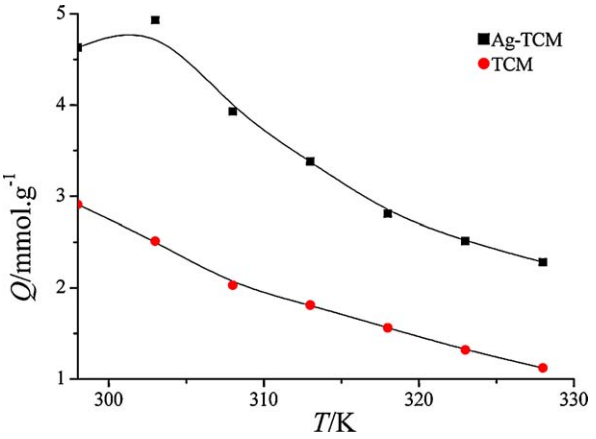

Fig. 8. Effects of temperature on adsorption of Ag^+ on adsorption capacity (pH 5; initial concentration, 20 mmol/L; contact time, 50 min).

Table 2
Thermodynamic parameters at different temperatures.

T (K)	ΔG (kJ/mol)	ΔH (kJ/mol)	ΔS (J/mol/K)
303	−15.66	−22.08	−21.18
313	−15.45		
323	−15.24		

addition, the speed and range of motion of Ag^+ become faster and wider, which increased the chance of adsorption.

However, when the temperature exceeded 30 °C, a higher temperature favored desorption or dechelation, which indicated that 30 °C was the optimal temperature for the adsorption of Ag(I) onto Ag-TCM.

The observed decrease in both values of $1/T$ and ln (Q_e/C_e) with elevated temperature indicates the exothermic nature of the adsorption process. The values of ln (Q_e/C_e) at different temperatures were treated according to Van't Hoff equation [48]:

$$\ln\left(\frac{Q_e}{C_e}\right) = \frac{-\Delta H}{RT} + \frac{\Delta S}{R},$$

where R is the universal gas constant (8.314 J/mol/K) and T is the absolute temperature (in Kelvin). Plotting ln (Q_e/C_e) against $1/T$ gives a straight line with slope and intercept equal to $-\Delta H/R$ and $\Delta S/R$, respectively.

The negative value of ΔH (Table 2) shows exothermic nature of adsorption process. Gibbs free energy of adsorption (ΔG) was calculated from the following relation:

$$\Delta G = \Delta H - T\Delta S$$

The negative value of ΔG (Table 2) indicates that the adsorption reaction is spontaneous. The observed decrease in negative values of ΔG with increasing temperature implies that the adsorption becomes less favorable at higher temperatures.

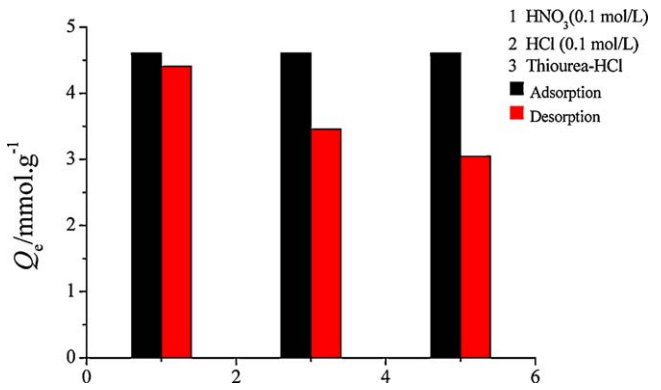

Fig. 9. The adsorption and desorption of Ag^+ from Ag-TCM in three eluents.

3.6. Evaluation of the selective adsorption

For the purpose of evaluating the selectivity of the beads, the selective adsorption studies were carried out under the optimum conditions. The results are shown in Table 3. Based on the results shown in Table 3, it can be seen that the adsorption capacity ratio of Ag-TCM for Ag(I) was 2.5 times greater than that of TCM. TCM can easily adsorb other ions as well as Ag^+, it demonstrates that the specific recognition cavities for Ag^+ created in Ag-TCM unlike TCM, which are developed by ion-imprinting. In the case of Ag-TCM, the cavities created after removal of the template were complementary to the imprint ion in size, shape and coordination geometries. It is evident that Ag-TCM has a strong ability to selectively adsorb Ag^+ from mixed metal ions in aqueous solution.

3.7. Effect of recycling adsorbents on Ag^+ adsorption

From practical point of view, repeated availability is a crucial factor for an advanced adsorbent [16,49,50]. Such adsorbent has higher adsorption capability as well as better desorption property which will reduce the overall cost for the adsorbent.

To evaluate the possibility of regeneration and reusability of Ag-TCM as an adsorbent, we performed the desorption experiments. Desorption of Ag^+ from Ag-TCM was demonstrated using three different eluents, namely 0.1 mol/L HCl, 0.1 mol/L HNO_3, and thiourea-HCl. It is found that the quantitative desorption efficiencies using HCl, and HNO_3 and thiourea-HCl were 95.1, 75.01 and 64%, respectively. The reusability was checked by following the adsorption–desorption process for three eluents, which are shown in Fig. 9. The 0.1 mol/L HNO_3 was the optimum eluent.

The effect of recycling times on the adsorption process was repeated 6 times, and the results are shown in Fig. 10. It is shown in Fig. 10 that the uptake capacity of Ag^+ on the adsorbents decreased slowly with increasing cycle number. The percentage adsorption remained steady at about 90% in the first five cycles, and then the uptake capacity of Ag^+ decreased. At the sixth regeneration cycle, the adsorption remained at 75%. These results show that the adsorbents can be recycled for Ag^+ adsorption with 0.1 mol/L HNO_3, and the adsorbents can be reused. The probable mechanism of the

Table 3
Selective determination.

Interfering ions	Adsorption capacity of Ag^+ (Q_1) (mmol/g)		Adsorption capacity of different ion (Q_2) (mmol/g)		K
	Ag-TCM	TCM	Ag-TCM	TCM	
Cd^{2+}	4.74	2.13	0.344	1.65	2.26
Zn^{2+}	4.56	2.03	0.506	2.75	2.25
Pb^{2+}	4.68	1.93	0.404	3.21	2.42
Cu^{2+}	4.60	1.78	0.482	2.42	2.61

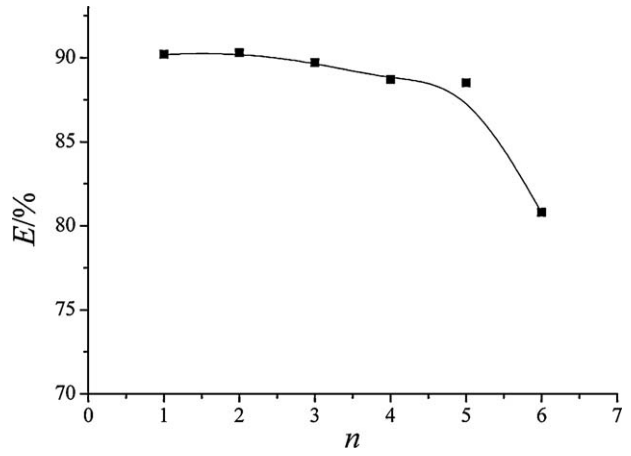

Fig. 10. Effect of recycling adsorbents on Ag^+ adsorption (pH 5; initial concentration, 20 mmol/L; temperature, 303 K; contact time, 50 min).

regeneration might be that in the first five cycles, both electrostatic and complexation reaction occurred between the HNO_3 and the metal ions; however, after five cycles, only electrostatic interaction prevailed.

4. Conclusions

In summary, the preferential adsorption of Ag(I) ions was successfully accomplished using Ag(I) imprinted magnetic thiourea-chitosan beads, the maximum adsorption capacity of Ag-TCM for Ag(I) was 4.93 mmol/g at pH 5.0, 30 °C. Adsorption of Ag(I) ions onto Ag-TCM followed the Langmuir adsorption isotherms. The kinetics of adsorption followed a pseudo-second order rate equation. An overall selectivity for Ag(I) ions was observed showing that Ag-TCM can be used effectively to remove and recover Ag(I) ions from aqueous solutions. It was also shown that Ag-TCM could be reused for 5 times. Ag-TCM was characterized by SEM, and BET–N_2 adsorption measurement. It is the author's hope that this result will be helpful for researchers who are interested in synthesizing and applying Ag-TCM as an alternative adsorbent in the separation, preconcentration and extraction of Ag(I) from aqueous solutions.

Acknowledgments

This work was supported by the Shandong Provincial Natural Science Foundation (Y2008B53) and Shandong Provincial Key Subject (Laboratory) Research Foundation (XTD0705).

References

[1] Y.C. Chang, S.W. Chang, D.H. Chen, Magnetic chitosan nanoparticles: studies on chitosan binding and adsorption of co(II) ions, React. Funct. Polym. 66 (2006) 335–341.
[2] M. Monier, D.M. Ayad, A.A. Sarhan, Adsorption of Cu(II), Co(II), and Ni(II) ions by modified magnetic chitosan chelating resin, J. Hazard. Mater. 177 (2010) 962–970.
[3] M. Monier, D.M. Ayad, A.A. Sarhan, Adsorption of Cu(II), Hg(II), and Ni(II) ions by modified natural wool chelating fibers, J. Hazard. Mater. 176 (2010) 348–355.
[4] A.B. dos Santos, F.J. Cervantes, J.B. van Lier, Review paper on current technologies for decolourisation of textile wastewaters: perspectives for anaerobic biotechnology, Bioresour. Technol. 98 (2007) 2369–2385.
[5] M. Kornaros, G. Lyberatos, Biological treatment of wastewaters from a dye manufacturing company using a trickling filter, J. Hazard. Mater. 136 (2006) 95–102.
[6] Y. Fu, T. Viraraghavan, Fungal decolorization of dye wastewaters: a review, Bioresour. Technol. 79 (2001) 251–262.
[7] J. Gao, Q. Zhang, K. Su, R. Chen, Y. Peng, Biosorption of acid yellow 17 from aqueous solution by non-living aerobic granular sludge, J. Hazard. Mater. 174 (2010) 215–225.
[8] S. Karcher, A. Kornmüller, M. Jekel, Screening of commercial sorbents for the removal of reactive dyes, Dyes Pigments 51 (2001) 111–125.
[9] S. Karcher, A. Kornmüller, M. Jekel, Anion exchange resins for the removal of reactive dyes from textile wastewaters, Water Res. 36 (2002) 4717–4724.
[10] M. Wawrzkiewicz, Z. Hubicki, Removal of tartrazine from aqueous solutions by strongly basic polystyrene anion exchange resins, J. Hazard. Mater. 164 (2009) 502–509.
[11] M. Wawrzkiewicz, Z. Hubicki, Equilibrium and kinetic studies on the sorption of acidic dye by macro porous anion exchange, Chem. Eng. J. 157 (2010) 29–34.
[12] Y.T. Zhou, H.L. Nie, C. Branford-White, Z.Y. He, L.M. Zhu, Removal of Cu^{2+} from aqueous solution by chitosan-coated magnetic nanoparticles modified with α-ketoglutaric acid, J. Colloid Interface Sci. 330 (2009) 29–37.
[13] S.S. Banerjee, D.H. Chen, Fast removal of copper ions by gum arabic modified magnetic nano-adsorbent, J. Hazard. Mater. 147 (2007) 792–799.
[14] S.H. Huang, D.H. Chen, Rapid removal of heavy metal cations and anions from aqueous solutions by an amino-functionalized magnetic nano-adsorbent, J. Hazard. Mater. 163 (2009) 174–179.
[15] C.L. Chen, X.K. Wang, M. Nagatsu, Europium adsorption on multiwall carbon nanotube/iron oxide magnetic composite in the presence of polyacrylic acid, Environ. Sci. Technol. 43 (2009) 2362–2367.
[16] C. Chen, J. Hu, D. Shao, J. Li, X. Wang, Adsorption behavior of multiwall carbon nanotube/iron oxide magnetic composites for Ni(II) and Sr(II), J. Hazard. Mater. 164 (2009) 923–928.
[17] J. Hu, D. Shao, C. Chen, G. Sheng, J. Li, X. Wang, M. Nagatsu, Plasma-induced grafting of cyclodextrin onto multiwall carbon nanotube/iron oxides for adsorbent application, J. Phys. Chem. B 114 (2010) 6779–6785.
[18] L.C.A. Oliveira, D.I. Petkowicz, A. Smaniotto, S.B.C. Pergher, Magnetic zeolites: a new adsorbent for removal of metallic contaminants from water, Water Res. 38 (2004) 3699–3704.
[19] J.F. Liu, Z.S. Zhao, G.B. Jiang, Coating Fe_3O_4 magnetic nanoparticles with humic acid for high efficient removal of heavy metals in water, Environ. Sci. Technol. 42 (2008) 6949–6954.
[20] M. Ozmen, K. Can, G. Arslan, A. Tor, Y. Cengeloglu, M. Ersoz, Adsorption of Cu(II) from aqueous solution by using modified Fe_3O_4 magnetic nanoparticles, Desalination 254 (2010) 162–169.
[21] Y.T. Zhou, C. Branford-White, H.L. Nie, L.M. Zhu, Adsorption mechanism of Cu^{2+} from aqueous solution by chitosan-coated magnetic nanoparticles modified with α-ketoglutaric acid, Colloids Surf. B: Biointerfaces 74 (2009) 244–252.
[22] K. Fujiwara, A. Ramesh, T. Maki, H. Hasegawa, K. Ueda, Adsorption of platinum(IV), palladium (II) and gold (III) from aqueous solutions onto l-lysine modified crosslinked chitosan resin, J. Hazard. Mater. 146 (2007) 39–50.
[23] P. Chassary, T. Vincent, E. Guibal, Metal anion sorption on chitosan and derivative materials: a strategy for polymer modification and optimum use, React. Funct. Polym. 60 (2004) 137–149.
[24] E. Guibal, N. Von Offenberg Sweeney, T. Vincent, J.M. Tobin, Sulfur derivatives of chitosan for palladium sorption, React. Funct. Polym. 50 (2002) 149–163.
[25] A. Ramesh, H. Hasegawa, W. Sugimoto, T. Maki, K. Ueda, Adsorption of gold(III) platinum(W) and palladium(II) onto glycine modified crosslinked chitosan resin, Bioresour. Technol. 99 (2008) 3801–3809.
[26] A.P. Zhu, M.B. Chan-Park, S. Dai, L. Li, The aggregation behavior of *o*-carboxymethyl chitosan in dilute aqueous solution, Colloids Surf. B: Biointerfaces 43 (2005) 143–149.
[27] R. Schmuhl, H. Krieg, M. Keizer, Adsorption of Cu (II) and Cr(VI) ions by chitosan: kinetics and equilibrium studies, Water SA 27 (2001) 1–7.
[28] Y. Yan, C. Chen, B.R.R.X. Wang, Studies of properties and preparation of chitosan resin cross-linked by formaldehyde and epichlorohydrin, Polym. Mater. Sci. Eng. 20 (2004) 53–57 (in Chinese with English abstract).
[29] B.J. Liu, D.F. Wang, H.Y. Li, Y. Xu, L. Zhang, As(III) removal from aqueous solution using α-Fe_2O_3 impregnated chitosan beads with As(III) as imprinted ions, Desalination 272 (2011) 286–292.
[30] B. Claude, L.C. Viron, K. Haupt, P. Morin, Synthesis of a molecularly imprinted polymer for the solid-phase extraction of betulin and betulinic acid from plane bark, Phytochem. Anal. 21 (2010) 180–185.
[31] P. Metilda, K. Prasad, R. Kala, J.M. Gladis, R.T. Prasada, G.R.K. Naidu, Ion imprinted polymer based sensor for monitoring toxic uranium in environmental samples, Anal. Chim. Acta 582 (2007) 147–153.
[32] S. Daniel, G.J. Mary, R.T. Prasada, Synthesis of imprinted polymer material with. Palladium ion nanopores and its analytical application, Anal. Chim. Acta 488 (2003) 173–182.
[33] R. Say, E. Birlik, A. Ersöz, F. Yılmaz, T. Gedikbey, A. Denizli, Preconcentration of copper on ion-selective imprinted polymer microbeads, Anal. Chim. Acta 480 (2003) 251–258.
[34] S.L. Sun, A.Q. Wang, Adsorption properties and mechanism of cross-linked. carboxymethyl-chitosan resin with Zn(II) as template ion, React. Funct. Polym. 66 (2006) 819–826.
[35] A. Ersöz, R. Say, A. Denizli, Ni(II) ion-imprinted solid-phase extraction and preconcentration in aqueous solutions by packed-bed columns, Anal. Chim. Acta 502 (2004) 91–97.
[36] T. Rosatzin, L.I. Andersson, W. Simon, K. Mosbach, Preparation of Ca^{2+} selective sorbents by molecular imprinting using polymerisable ionophores, J. Chem. Soc. Perk. Trans. 2 (28) (1991) 1261–1265.
[37] P.K. Dhal, F.H. Arnold, Template-mediated synthesis of metal-complexing. Polymers for molecular recognition, J. Am. Chem. Soc. 113 (1991) 7417–7418.
[38] L. Zhou, et al., Adsorption of platinum(IV) and palladium(II) from aqueous solution by thiourea-modified chitosan microspheres, J. Hazard. Mater. 172 (2009) 439–446.

[39] X. Luo, et al., Removal of water-soluble acid dyes from water environment using a novel magnetic molecularly imprinted polymer, J. Hazard. Mater. 187 (2011) 274–282.
[40] B. Salih, Synthesis of 1,4,8,11-tetraaza-cyclo-tetradecane monomer by addition of acryloyl chloride and its polymer for specific transition metal binding, J. Appl. Polym. Sci. 83 (2002) 1406–1414.
[41] S.L. Sun, A.Q. Wang, Adsorption properties of carboxymethyl-chitosan and crosslinked carboxymethyl-chitosan resin with Cu(II) as template ions, Sep. Purif. Technol. 49 (2006) 197–204.
[42] Y.S. Ho, G. McKay, A comparison of chemisorption kinetic models applied to pollutant removal on various sorbents, Proc. Saf. Environ. Protect. 76 (1998) 332–340.
[43] G. Crini, Kinetic and equilibrium studies on the removal of cationic dyes from aqueous solution by adsorption onto a cyclodextrin polymer, Dyes Pigments 77 (2008) 415–426.
[44] G. Crini, H.N. Peindy, F. Gimbert, C. Robert, Removal of C.I. basic green 4 (malachite green) from aqueous solutions by adsorption using cyclodextrin based adsorbent: kinetic and equilibrium studies, Sep. Purif. Technol. 53 (2007) 97–110.
[45] Y. Ho, G. McKay, Pseudo-second order model for sorption processes, Process Biochem. 34 (1999) 451–465.
[46] A.Z.M. Badruddoza, Goh Si Si Hazel, K.M.S. Hidajat, M.S. Uddin, Synthesis of carboxymethyl-cyclodextrin conjugated magnetic nano-adsorbent for removal of methylene blue, Colloids Surf. A: Physicochem. Eng. Asp. 367 (2010) 85–95.
[47] B. Hameed, A. Ahmed, K. Latiff, Adsorption of basic dye (methylene blue) onto activated carbon prepared from rattan sawdust, Dyes Pigments 75 (2007) 143.
[48] A. Atia, A.M. Donia, H.A. El-Boraey, D.H. Mabrouk, Adsorption of Ag(I) on glycidyl methacrylate/*N*,*N*-methylene bis-acrylamide chelating resins with embedded iron oxide, Sep. Purif. Technol. 48 (2006) 281–287.
[49] C. Chen, X. Wang, Adsorption of Ni(II) from aqueous solution using oxidized multiwall carbon nanotubes, Ind. Eng. Chem. Res. 45 (2006) 9144–9149.
[50] G. Sheng, S. Wang, J. Hu, Y. Lu, J. Li, Y. Dong, X. Wang, Adsorption of Pb(II) on diatomite as affected via aqueous solution chemistry and temperature, Colloids Surf. A: Physicochem. Eng. Asp. 339 (2009) 159–166.